Interleukin 1 (IL-1) Causes Changes in Lateral and Rotational Mobilities of IL-1 Type I Receptors†

Chunmei Guo,‡,§ Katy E. Georgiadis,‡,|| Steven K. Dower,⊥ David Holowka,*,‡ and Barbara A. Baird*,‡

Department of Chemistry and Chemical Biology, Baker Laboratory, Cornell University, Ithaca, New York 14853-1301, and Department of Medicine and Pharmacology, University of Sheffield Medical School, Royal Hallamshire Hospital, Sheffield S10-2JF, U.K.

Received August 26, 1998; Revised Manuscript Received November 19, 1998

ABSTRACT: To investigate IL-1-dependent interactions of IL-1 type I (IL-1 RI) receptors on intact cells, lateral and rotational mobilities and detergent insolubility were investigated. Lateral mobility was measured by fluorescence photobleaching recovery, using a Cy3-modified, noncompetitive mAb specific for IL-1RI (M5) bound to wild-type IL-1 RI or mutant IL-1 RI with a truncated cytoplasmic tail. Addition of IL-1 causes significant reduction in the mobile fraction of wild-type IL-1 RI for two different transfected cell lines. For the mutant IL-1 RI, no significant decrease in response to IL-1 is observed, indicating that the missing cytoplasmic segment is involved in IL-1-dependent interactions of IL-1 RI that lead to reduced lateral mobility on the cell surface. The rotational mobility of IL-1 RI was assessed with phosphorescence anisotropy decay measurements using erythrosin-labeled M5. IL-1 decreases the rotational mobility of cell surface IL-1 RI on the microsecond time scale and also increases the initial anisotropy, indicating loss in segmental motion. Measurements of resistance to solubilization by Triton X-100 showed that IL-1 binding increases the fraction of IL-1 RI sedimenting with cytoskeletal residues. The IL-1 receptor antagonist protein (IL-1ra) causes partial effects in reducing rotational mobility and increasing detergent insolubility of M5-lableled IL-1 RI, indicating that this ligand causes structural changes in the presence of the dimerizing M5 mAb. These ligand-dependent physical interactions of IL-1 RI on the cell surface may be related to signal initiation by this receptor.

Interleukin 1 (IL-1)[1] is a major class of cytokines that mediate pleiotropic immune and inflammatory responses (*1*, *2*) including antibody synthesis (*3*), T cell activation (*4*), and synthesis and secretion of acute-phase proteins, prostaglandins, and collagenase (*5*). The IL-1 family includes two agonists, IL-1α and IL-1*β*, and one antagonist, IL-1ra polypeptides (*6*−*8*). Two types of IL-1 receptors have been characterized: type I IL-1 receptors (IL-1 RI) mediate transmembrane signaling (*9*, *10*). Type II IL-1 receptors (IL-1 RII) do not, but may act as decoys to regulate IL-1 RI-mediated responses (*10*, *11*). Because of intensive research on these molecules during the past decade, good progress has been made in understanding the intracellular signal transduction pathways that they activate (*12*).

Both IL-1 RI and IL-1 RII have a single transmembrane polypeptide chain (*13*−*15*) and an extracellular segment responsible for IL-1 binding that consists of three immunoglobulin-like domains. IL-1 RI has a substantially longer cytoplasmic segment (219 residues; *13*, *14*) than IL-1 RII (29 residues; *15*). The cytoplasmic domain of IL-1 RI has a sequence that is homologous with the *Drosophila* gene product Toll (*16*), but not with known protein kinases (*17*). Several studies showed that the cytoplasmic domain of IL-1 RI is required for IL-1 signal transduction (*18*−*20*). Recently, a receptor-associated serine/threonine kinase activity was identified that appears to be important for NF-*κ*B activation (*21*). These results suggest that the cytoplasmic segment of IL-1 RI interacts with other protein components to transduce a signal. Chemical cross-linking studies also provided evidence for IL-1-dependent interactions of IL-1 RI with other cellular proteins, including a homologous polypeptide, the receptor accessory protein (*22*, *23*).

Our recent fluorescence resonance energy transfer (FRET) measurements showed that IL-1 binding causes IL-1 RI self-aggregation which correlates with the initiation of cellular signaling (*24*). For this study, a noncompetitive, nonactivating mAb specific for IL-1RI, M5, was used to introduce fluorescent probes. IL-1α and IL-1*β* cause a time- and temperature-dependent increase in FRET that occurs both

† Supported in part by NSF Grant GER-9023463, NIH Grants AI18306 and GM07273 (C.G.), and an Arthritis Foundation Postdoctoral Fellowship (K.E.G.).

* Corresponding authors. Telephone: (607) 255-4095. Fax: (607) 255-4137. E-mail: bab13@cornell.edu.

‡ Cornell University.

§ Present address: Division of Pharmacology and Toxicology, University of Texas at Austin, Pharmacy Building, Austin, TX 78712.

|| Present address: Department of Biomedical Engineering/Wb3, Cleveland Clinic Foundation, 9500 Euclid Ave., Cleveland, OH 44195.

⊥ Royal Hallamshire Hospital.

[1] Abbreviations: IL-1, interleukin 1; IL-1ra, interleukin 1 receptor antagonist; IL-1 RI, interleukin 1 type I receptor; IL-1 RII, interleukin 1 type II receptor; ErITC, erythrosin 5-isothiocyanate; FITC, fluorescein 5-isothiocyanate; FRET, fluorescence resonance energy transfer; MEM, modified Eagle's medium; PBS, phosphate-buffered saline; CHO-mu1c, CHO-K1 cells transfected with wild-type IL-1 RI; CHO-extn, CHO-K1 cells transfected with IL-1 RI with truncated cytoplasmic tail; C-127, a mouse mammary carcinoma cell line transfected with wild-type IL-1 RI; mAb, monoclonal antibody; HBS, HEPES-buffered saline; PGE2, prostaglandin E2; FPR, fluorescence photobleaching recovery.

10.1021/bi982068l CCC: $18.00
Published on Web 01/14/1999

with the wild-type receptor and with a mutant receptor lacking the cytoplasmic tail, indicating that the self-aggregation detected is not a consequence of signaling events. These measurements could not ascertain whether interactions with other cellular components accompany IL-1-dependent receptor self-aggregation.

In the study presented, we investigated physical interactions of IL-1 RI with other cellular components on intact cells. Phosphorescence anisotropy and fluorescence photobleaching recovery (FPR) measurements show that the rotational and lateral mobility of IL-1 RI decreases significantly upon IL-1 binding. These results, together with the observation of induced detergent insolubility, provide physical evidence that IL-1 binding causes receptors to form aggregates larger than dimers that involve interactions with other detergent-resistant structures.

EXPERIMENTAL PROCEDURES

Materials. Erythrosin 5-isothiocyanate (ErITC) and fluorescein 5-isothiocyanate (FITC) were purchased from Molecular Probes, Inc. (Eugene, OR). Glucose oxidase (180 000 Sigma units/mg) was purchased from Sigma Chemical Co. (St. Louis, MO). Argon was prepurified grade (O_2 < 5 ppm). Cy3 was purchased from Biological Detection Systems (Pittsburgh, PA). Recombinant IL-1α, IL-1ra, and M5, the rat mAb specific for IL-1 RI, were produced and purified (*25*−*27*), and their binding with IL-1 RI was characterized (*24*) as described.

Cells. CHO-K1 cells stably transfected with wild-type IL-1 RI (CHO-mu1c), and with IL-1 RI with a truncated cytoplasmic tail (CHO-extn) (*18*), were maintained in Ham's F-12 medium. C-127 mouse mammary carcinoma cells stably transfected with wild-type IL-1 RI (*28*) were maintained in Dulbecco's MEM medium. These media were supplemented with 10% fetal bovine serum, 100 units/mL penicillin, 100 μg/mL streptomycin, and 250−500 μg/mL Geneticin in a humidified atmosphere of air enriched with 5.6% CO_2. The cells were harvested at confluence with 1.5 mM EDTA in a saline/HEPES buffer, sedimented at 180*g* for 5 min, and resuspended to a density of 3×10^6 cells/mL in HEPES-buffered saline (HBS: 135 mM NaCl, 5 mM KCl, 1.8 mM $CaCl_2$, 1 mM $MgCl_2$, 5.6 mM glucose, and 20 mM HEPES, pH 7.4, with 1 mg/mL bovine serum albumin).

Labeled Derivatives. IL-1α and M5 were labeled with ^{125}I using the chloramine T method (*29*). The Cy3 and FITC derivatives of M5 were prepared and characterized as described (*24*). For the ErITC derivative, M5 (1 mg/mL) in PBS/EDTA, pH 7.7 (10 mM sodium phosphate, 100 mM NaCl, and 1 mM EDTA), was incubated at room temperature in the dark for 12 h after addition of 30 mM ErITC in DMSO to give a 5:1 molar ratio of ErITC to M5. The sample was then microfuged at 9000*g* for 10 min at 4 °C, and the supernatant was exhaustively dialyzed in PBS/EDTA at pH 7.4. The molar ratio of coupling, ErITC:M5, was estimated to be 4:1 in two preparations as based on extinction coefficients of 83 000 M^{-1} cm^{-1} (536 nm) for ErITC, 31 600 M^{-1} cm^{-1} (280 nm) for ErITC, and 210 000 M^{-1} cm^{-1} (280 nm) for M5.

Detergent Insolubility Experiments. CHO-mu1c cells (5×10^6/mL) in HBS were incubated with ^{125}I-M5 (10 nM) or ^{125}I-IL-1 for 50 min at 22 or 4 °C, as indicated, and washed once with HBS. Nonspecific binding, determined with excess unlabeled ligand, was less than 5% of the total bound label and was corrected in the data shown. As indicated, M5, IL-1α, IL-1β, or IL-1ra was incubated with the labeled cells for 50 min at 22 or 4 °C and then washed with HBS. In some experiments, the washed cells were subsequently labeled with goat anti-rat IgG for 2 h at 4 °C. The treated cells were sedimented and then lysed by resuspension (5×10^6 cells/mL) for 10 min on ice in lysis buffer [10 mM Tris, pH 6.5, 50 mM NaCl, 5 mM EDTA, 0.01% NaN_3, 0.05% Triton X-100, 0.02 unit/mL aprotinin, and 1 mg/mL 4-(2-aminoethyl)benzenesulfonylfluoride]. In some experiments, the concentration of Triton X-100 in the lysis buffer was varied as indicated. The amount of insoluble ^{125}I-labeled IL-1 RI was determined as a percent of the specifically bound ^{125}I counts that sedimented after centrifuging the lysed cells at 10000*g* for 3 min and counting pellets and supernatants in a Beckman 9000 gamma counter. Similar trends in the data were obtained when the lysed cells were centrifuged at 180*g* for 5 min.

Lateral Diffusion Measurements. FPR was measured with previously established methods (*30*) using the 514 nm line of an argon ion laser as the source for both bleaching and monitoring the fluorescence recovery of the Cy3-M5 probe. The e^{-2} radius of the illuminated spot was measured to be 0.78 μm on a Mylar film with a sensitive CCD camera. No detectable photobleaching was caused by the monitor beam.

Cells were resuspended at 8×10^6 cells/mL in HBS and incubated with a saturating amount (10−30 nM) of Cy3-M5 mAb for 40 min at 4 °C; then the mixture was washed with fresh buffer and divided into two samples. IL-1 was added to one sample and incubated for 30 min, and no addition was made to a control sample. FPR was measured on the plasma membranes of single cells at ambient temperature (∼22 °C) with a Zeiss universal microscope. The percent mobile fraction, %*R*, and the lateral diffusion coefficient, *D*, were obtained by fitting the FPR recovery curve according to Yguerabide et al. (*31*):

$$\%R = (F_\infty - F_0)/(F_i - F_0) \quad (1)$$

$$D = (w^2/4t_{1/2})\beta \quad (2)$$

where F_i is the fluorescence before the bleach, F_0 is the fluorescence immediately after bleach, and F_∞ is the fluorescence after recovery; *w* is the radius of the focused laser beam, $t_{1/2}$ is the half-time for recovery, and β is a tabulated parameter that depends on the percent of bleach (*31*).

Rotational Diffusion Measurements. Time-dependent phosphorescence anisotropy was measured on suspended cells with the instrumentation described previously (*32*, *33*). Erythrosin 5-isothiocyanate conjugated to M5 (ErITC-M5) was excited with the 532 line of a frequency-doubled Nd:YAG laser (Quanta-Ray DCR-2A) that was polarized with a Glan Thompson prism. In L-format, collection of vertically polarized emission was followed by collection of horizontally polarized emission and signal-averaged (*34*); typically, 10 000 decays were accumulated in 1000 s for each component. After correction for any changes in laser power during emission collection, nonspecific phosphorescence was corrected by subtracting the decay of the nonspecific control sample. The difference intensity [$d(t)$; eq 3], total intensity

[$S(t)$; eq 4], and anisotropy [$r(t)$; eq 5] were calculated according to (*35*):

$$d(t) = I(t)_{II} - gI(t)_{\perp} \quad (3)$$

$$S(t) = I(t)_{II} + ghI(t)_{\perp} \quad (4)$$

$$r(t) = d(t)/S(t) \quad (5)$$

in which $I(t)_{II}$ is the parallel polarized phosphorescence intensity and $I(t)_{\perp}$ is the perpendicular polarized phosphorescence intensity. The *g*-factor was determined to be 1.01 for the L-format configuration (*32*). The aperture correction, *h*, has a value of 1.75 in our system (*33*). For all the experiments, the anisotropy decays were fit between 15 and 200 μs with a single-exponential decay using a weighted nonlinear least-squares fitting routine (*33*):

$$r(t) = a + b\exp(-t/\phi) \quad (6)$$

in which $r(t)$ is the time-dependent phosphorescence anisotropy decay (eq 5), ϕ is the rotational correlation time, and a is the residual anisotropy (r_∞). The sum $a + b$ yields the initial anisotropy (r_0).

Dissociation of Receptor-Bound FITC-IL-1α. Cells were first incubated with saturating concentrations of FITC-IL-1α (30 nM for 3×10^6 C-127 cells/mL) for 50 min at 22 °C. A Coulter Epics Profile flow cytometer was used to determine the mean fluorescence intensity on cells. After the cell-associated fluorescence reached a steady state, FITC-IL-1α dissociation was initiated by centrifugation of the cells for 3 min at 1500*g*, followed by resuspension in HBS twice. The decrease in cell-associated FITC fluorescence was monitored by flow cytometry after washing. Nonspecific binding and cell autofluorescence were assessed in parallel samples by addition of fluorescently labeled ligands after blocking the receptors with a 20-fold excess of unlabeled over labeled IL-1α.

RESULTS

Lateral Mobility of IL-1 RI. The M5 mAb binds to murine IL-1 RI at a site that is distinct from the IL-1 site, and does not interfere with the capacity of IL-1 to bind and stimulate responses in EL-4 cells (*26*). Although M5 alone does not trigger a detectable cellular response, it probably cross-links IL-1 RI to form dimers at the cell surface (*36*). Our previous flow cytometry experiments established that the FITC and Cy3 derivatives of M5 bind to transfected murine IL-1 RI on CHO-K1 cells and on C-127 cells with the same properties as the ^{125}I derivative of M5 (*24*, *25*). With fluorescence microscopy and steady-state fluorescence spectroscopy to detect endocytosis-mediated quenching due to acidification in endosomes, we established that >95% of IL-1 RI labeled by these fluorescent M5 derivatives remains at the cell surface under the conditions of our experiments in the presence or absence of IL-1 ligands (*37*). Thus, we could use these fluorescent M5 to monitor diffusion of IL-1 RI in the plasma membrane.

For FPR measurements of lateral diffusion, CHO or C-127 cells were labeled with a saturating amount of Cy3-M5 mAb and washed, and then IL-1β was added or not added. Figure 1 displays the FPR results for C-127 cells with (○) or without (■) IL-1 bound, in terms of mobile fraction (percent recovery, %*R*) and diffusion coefficient (*D*). Each point represents an individual cell measurement. In the absence of IL-1, the average values for *D* and %*R* are 5.7×10^{-10} cm^2/s and 64%, respectively (Table 1), which are in the range found for many cell surface proteins (*38*). In the presence of 10 nM IL-1 (~90% saturation of IL-1 RI), there is a significant decrease in the mobile fraction to 46% (Figure 1; Table 1). The average *D* for the Cy3-M5-labeled IL-1 R1 that remain mobile when IL-1 is bound does not change significantly (5.2×10^{-10} cm^2/s; Figure 1, Table 1). Under the conditions of these FPR measurements, our previous resonance energy transfer measurements showed that IL-1 causes IL-1 RI to aggregate (*24*). The decrease in %*R* resulting from IL-1 binding cannot be simply explained by the increased molecular mass of IL-1 RI dimers or small oligomers. Rather, it appears that there are more extensive interactions with other cellular components.

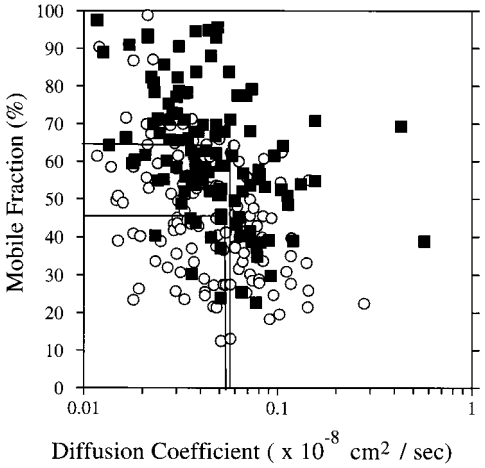

FIGURE 1: FPR measurements of IL-1 RI lateral motility on C-127 cells. Data are represented as mobile fraction (%*R*) vs diffusion coefficient (*D*) for 123 measurements on individual cells in 5 separate experiments. Cy3-M5-labeled cells were treated (○) or not treated (■) with 10 nM IL-1β for 30 min at 4 °C prior to measurement at 22 °C. The lines indicate the average values of *D* and %*R* for the different samples.

Table 1: Summary of FPR Results for IL-1RI

	D ($\times 10^{-10}$ cm^2/s)		%*R*	
cells	−IL-1	+IL-1	−IL-1	+IL-1
C-127 ($n = 123$)[b]	5.7 ± 0.6[a]	5.2 ± 0.3	64 ± 2	46 ± 2
CHO-mu1c ($n = 53$)	12.2 ± 1	12.5 ± 1	74 ± 4	60 ± 3
CHO-extn ($n = 50$)	9.9 ± 1	10.0 ± 1	58 ± 3	53 ± 3

[a] Standard error of the mean. [b] *n*: Number of FPR measurements.

To determine whether the cytoplasmic segment of IL-1 RI is involved, we compared FPR measurements for wild-type IL-1 RI and a mutant IL-1 RI with truncated cytoplasmic tail. These were examined in CHO-K1 cell transfectants, designated CHO-mu1c and CHO-extn cells, respectively. The average *D* for wild-type receptors on CHO-mu1c cells in the absence of IL-1 is 12.2×10^{-10} cm^2/s with an average mobile fraction of 74% [Figure 2A (■), Table 1]. This value of *D* is 2-fold larger than that observed for the C-127 cells, but still within the range observed for various cell surface proteins (*39*). When IL-1 is added to the cells, the average %*R* decreases to 60% [Figure 2A (○), Table 1], similar to the decrease observed for the C-127 cells (Figure 1, Table 1). The average value of *D* did not show a significant change

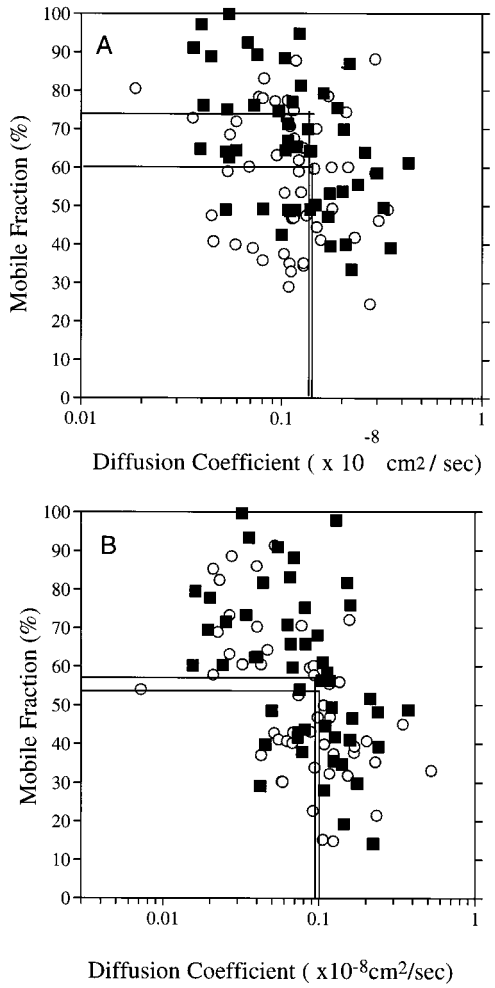

FIGURE 2: Lateral mobility measurements of wild-type IL-1 RI on CHO-mu1c cells (A) and mutant IL-1 RI with truncated cytoplasmic tail on CHO-extn cells (B). Mobile fraction (%*R*) vs diffusion coefficient (*D*) are plotted for 50 measurements made at 22 °C on individual cells of each type in at least 3 separate experiments. Cy3-M5-labeled cells were treated (○) or not treated (■) with 3 nM IL-1β for 30 min at 4 °C prior to measurement at 22 °C. The lines indicate the average values of *D* and %*R* for the different samples.

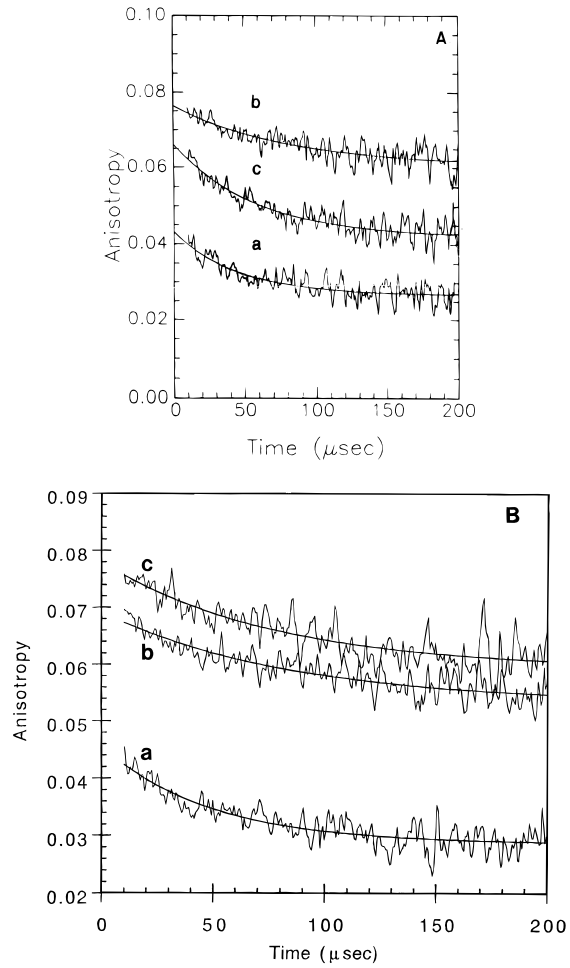

FIGURE 3: Phosphorescence anisotropy measurements of rotational mobility of ErITC-M5-IL-1 RI complexes on C-127 cells, measured at 22 °C. (A) Effects of IL-1α compared to IL-1ra on the same sample of labeled cells: (a) representative anistotropy decay curve with no additions; (b) decay curve after the addition of 30 nM IL-1α; (c) decay curve after the addition of 30 nM IL-1ra. (B) Effects of incubating with IL-1 and then washing to remove weakly bound population, on the same sample of labeled cells: (a) anisotropy decay curve before addition of IL-1; (b) decay curve after incubation with 1.6 nM IL-1α; (c) decay curve after subsequent wash to remove weakly bound IL-1. The smooth lines through the data represent fits to eq 6. Values for the fitting parameters for panel A are (curve a) $r_0 = 0.043$, $r_\infty = 0.027$, $\phi = 44.9$ μs; (curve b) $r_0 = 0.076$, $r_\infty = 0.060$, $\phi = 80.3$ μs; (curve c) $r_0 = 0.066$, $r_\infty = 0.042$, $\phi = 57.1$ μs. Values for the fitting parameters for panel B are (curve a) $r_0 = 0.043$, $r_\infty = 0.029$, $\phi = 48$ μs; (curve b) $r_0 = 0.069$, $r_\infty = 0.053$, $\phi = 82$ μs; (curve c) $r_0 = 0.078$, $r_\infty = 0.059$, $\phi = 75$ μs.

after addition of IL-1, as for the C-127 cells. For CHO-extn cells transfected with cytoplasmic tail-truncated IL-1 RI, the average values for *D* and %*R* are 9.9×10^{-10} cm^2/s and 58%, and these values are not significantly altered by the addition of IL-1 [Figure 2B (○), Table 1]. Thus, it appears that the cytoplasmic segment of IL-1 RI participates in IL-1-dependent interactions with other cellular components that result in reduced lateral mobility of this complex.

Rotational Mobility of IL-1 RI. Rotational motion within the plasma membrane is expected to be more sensitive than lateral motion to changes in the effective size of labeled proteins, and thereby their state of aggregation (*39*). We assessed rotational mobility on the microsecond time scale by measuring the time-dependent phosphorescence anisotropy decay of ErITC-M5 bound to IL-1 RI. Phosphorescence emission from ErITC arises from an excited triplet state, and the observed emission usually contains multiple components. In our measurement at 22 °C, the total intensity decay was resolved into three components, with normalized amplitudes and lifetimes, respectively, of 0.14 and 18 μs, 0.27 and 63 μs, and 0.59 and 150 μs (data not shown).

A representative phosphorescence anisotropy decay curve for ErITC-M5 bound to IL-1 RI on C-127 cells in the absence of IL-1 is shown in Figure 3A, curve a. As in all of the experiments described, the anisotropy decay can be fit by the initial anisotropy r_0, the residual anisotropy r_∞, and a single rotational correlation time, ϕ (eq 6), in the microsecond time regime observed. Four experiments carried out under the conditions of Figure 3A, curve a, yielded an average value of $\phi = 42 \pm 8$ μs (Table 2). This time is longer than expected for a membrane protein with only one or two transmembrane segments (monomer or dimer of IL-1 RI) rotating in a fluid bilayer, suggesting that the rotational freedom is restricted even in the absence of IL-1. The nonzero value of r_∞ (0.026) indicates that some of the ErITC-M5-IL-1 RI complexes do not fully depolarize on the time scale of these measurements.

Table 2: Summary of Phosphorescence Anisotropy Results for IL-1RI

treatment	r_0	r_∞	ϕ (μs)
ErITC-M5 ($n = 4$)[b]	0.043 ± 0.004[a]	0.026 ± 0.003	42 ± 8
+IL-1 ($n = 2$)	0.073 ± 0.004	0.057 ± 0.004	81 ± 1
+IL-1ra ($n = 2$)	0.063 ± 0.004	0.040 ± 0.003	65 ± 12

[a] Standard deviation. [b] n: Number of experiments.

Incubation of the initial sample corresponding to Figure 3A, curve a, with a saturating dose of IL-1α (30 nM) yielded the trace shown in Figure 3A, curve b. As summarized in Table 2, r_0 for the sample with IL-1 bound is consistently higher than that observed in the absence of IL-1. The r_0 value for the observed microsecond anisotropy decay approximates the r_∞ value for the anistropy decay occurring on the nanosecond time scale during which segmental motion is expected to occur. The differential r_0 values indicate that there is a component to the anisotropy decay with a correlation time on the submicrosecond time scale that rotates more freely in the absence of IL-1. This suggests that the M5-IL-1 RI complex has less segmental flexibility when IL-1 is bound. The r_∞ value in the microsecond time regime is also consistently higher for the sample with IL-1, suggesting that a larger fraction of the IL-1 RI is rotationally immobile. The observed anisotropy decay for the sample with IL-1 has $\phi = \sim 80$ μs, consistent with the view that mobile IL-1 RI complexes with IL-1 rotate at a rate that is roughly half of that for the receptors with no IL-1 bound. The remainder exhibit no significant rotation on this time scale.

When IL-1ra is added instead of IL-1 to saturate the M5-IL-1 R1, the respective r_0 and r_∞ values are consistently between those observed for the other two samples (Figure 3A, curve c, and Table 2). Comparison of the r_0 values suggests that, on average, segmental motion on the nanosecond time scale for M5-IL-1 R1 with IL-1ra bound is greater than that with IL-1 bound, but less than that without IL-1. This, together with the intermediate values of ϕ and r_∞ for the IL-1ra sample, is consistent with two populations of receptor complexes: one that is more similar to IL-1-receptor/M5 complexes, and one that is more similar to unliganded receptor/M5 complexes. Other explanations, such as a single population of IL-1ra-receptor/M5 complexes with intermediate rotational motion, are also possible.

Dependence of Receptor Aggregation on Readily Dissociable IL-1. In a different set of experiments, the anisotropy decay curves for ErITC-M5-IL-1 RI in the absence and presence of IL-1α (Figure 3B, curves a and b, respectively) were compared to cells incubated with saturating IL-1 and then washed (Figure 3B, curve c). Curve c is similar to curve b except that the r_0 and r_∞ values are slightly greater. The amount of IL-1α remaining bound to receptors under these wash conditions was assessed in parallel experiments using FITC-IL-1α as a probe. In two separate experiments, 64 ± 2% of the initially bound FITC-IL-1 remained bound after the wash steps. Thus, a large fraction of IL-1−receptor complexes bind tightly, and the readily dissociable IL-1 population is not necessary to maintain the interactions which cause the IL-1-dependent loss of IL-1 RI rotational motion. Our previous experiments showed that washing did not reverse IL-1-dependent FRET (*24*). These combined results support the view that IL-1-mediated IL-1 RI self-aggregation

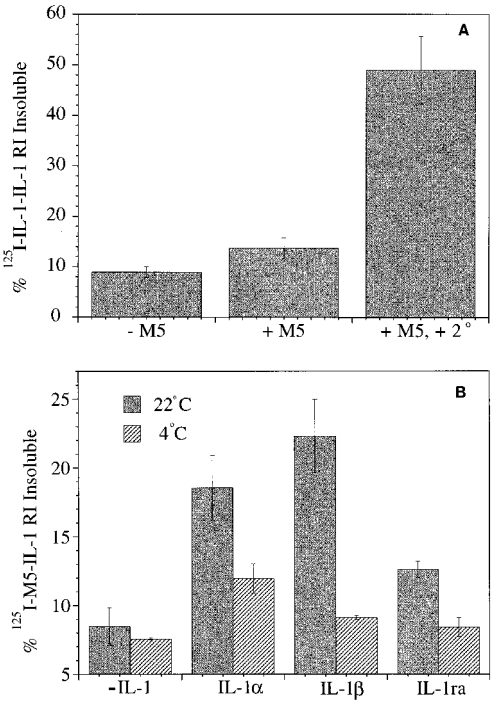

FIGURE 4: Detergent insolubility of IL-1 RI complexes on CHO-muc1 cells. (A) IL-1 RI labeled with ^{125}I-IL-1 and tested with M5. Cells (5×10^6/mL) were incubated with or without 5 nM M5 for 60 min at 4 °C, and one aliquot with M5 was subsequently washed and incubated with goat anti-rat IgG for 2 h at 4 °C. (B) IL-1 RI labeled with ^{125}I-M5 and tested with IL-1 ligands. Cells (5×10^6/mL) were incubated with no IL-1 or with 30 nM IL-1α, IL-1β, or IL-1ra for 60 min at either 22 °C (solid bars) or 4 °C (hatched bars). After sedimentation and resuspension in Triton X-100 lysis buffer, samples were centrifuged, and the supernatant and pellets were counted separately in a gamma counter to determine the percent of total radioactivity in the insoluble pellet.

results in stable complexes containing tightly bound IL-1 and possibly other cellular components.

Detergent Insolubility. Because of evidence for IL-1-dependent decreases in the lateral and rotational motion of IL-1RI, we tested the possibility that IL-1 or M5 causes receptors to interact with the detergent-resistant cellular cytoskeleton such that they sediment with the cytoskeletal residues after cell lysis. In separate experiments, either ^{125}I-M5 or ^{125}I-IL-1 was used to label the receptors, and then, after binding other ligands or no binding, cells were lysed with the nonionic detergent Triton X-100. In the representative experiment at 4 °C shown in Figure 4A, 9% of the ^{125}I-IL-1 bound to IL-1 RI on cells is insoluble in the absence of M5, and addition of M5 alone causes a small increase to 14%. Upon aggregation of IL-1 RI with M5 and a secondary antibody, a large increase in insolubility to 50% occurs. This increase is not due to the formation of large aggregates of immune complexes that sediment with IL-1 RI because no increase in the insoluble fraction occurs when the secondary antibody is added after cell lysis (data not shown). Thus, it appears that aggregation of IL-1 RI on the cell surface causes interactions leading to association with the cellular cytoskeleton.

As shown in Figure 4B, 5−10% of the receptors labeled with ^{125}I-M5 are insoluble in the absence of IL-1. However, binding of IL-1α or IL-1β at 22 °C results in significant increases in the percentage of receptors sedimenting with the cytoskeletal residues of the lysed cells. This IL-1-

dependent increase in detergent insolubility was observed consistently in 12 different experiments where the concentration of Triton X-100 was varied from 0.04% to 1%. The ratio of IL-1-dependent to IL-1-independent insolubility was similar over this range, but the magnitude of insolubility was somewhat greater at the lower concentrations (data not shown). Interestingly, IL-1ra causes a small but significant increase in the insolubility of the ^{125}I-M5-labeled IL-1 RI at 22 °C. At 4 °C, small or insignificant increases in IL-1 RI insolubility are caused by IL-1 ligands (Figure 4B). The observed temperature dependence, 22 °C vs 4 °C, and also the difference between the effects of IL-1α and IL-1β compared to IL-1ra at 22 °C are similar to IL-1-induced aggregation of IL-1 RI (*24*). These results from independent measurements of energy transfer (*24*), lateral (Figures 1 and 2) and rotational mobility (Figure 3), and detergent insolubility (Figure 4) suggest a relationship between the observed physical interactions that may also be related to function.

DISCUSSION

We previously observed IL-1-dependent IL-1 RI self-aggregation that correlated with signal initiation, and occurred in the absence of a full cellular response, suggesting that receptor aggregation is an early event in this process (*24*). Similar aggregation was detected with labeled anti-IL-1 R1 (M5) or with M5 Fab fragments as FRET probes, indicating that M5-induced receptor dimerization was not necessary. The FRET measurements did not allow determination of the fraction of IL-1 RI molecules that undergo aggregation, or whether this process leads to interactions with other cellular components. Although biochemical studies have provided evidence for IL-1-dependent IL-1 RI interactions with a kinase (*21*, *40*) and a polypeptide that is structurally homologous to IL-1 RI (*23*), the stoichiometries of these interactions are unknown. Furthermore, the lateral and rotational mobilities of this receptor before and after IL-1 engagement have not been previously investigated.

M5 binds tightly to IL-1 RI at the cell surface (*37*) and thus provides a means to label IL-1 RI specifically with radioactive or spectroscopic probes. Because IL-1 RI are normally expressed on most mammalian cells at very low densities that are insufficient for our spectroscopic measurements, we employed two different cell lines, C-127 and CHO-mu1c, that overexpress this receptor. The functional competence of transfected receptors in these cells has been previously established (*18*, *24*).

For our phosphorescence anisotropy measurements, only the more highly expressing C-127 cells provided an adequate signal-to-noise ratio. For these cells, we previously showed that IL-1α alone does not trigger prostaglandin E2 (PGE2) production, but it does trigger a significant response when M5 is also bound (*24*). For the CHO-muc1 cells, IL-1 stimulates a strong PGE2 response that is not affected by M5. These observations, suggesting that M5 synergizes with IL-1 to mediate signaling under suboptimal conditions, are consistent with our preliminary results that significant arachidonic acid production is stimulated by the IL-1 antagonist protein, IL-1ra, if M5 is also present (*37*).

The FPR measurements of IL-1 RI labeled with Cy3-M5 show that this receptor exhibits lateral diffusion coefficients that are within the range typical for plasma membrane proteins [$(6-12) \times 10^{-10}$ cm^2/s; Table 1]. These values can be compared with those observed at 21−23 °C for two other plasma membrane proteins with single transmembrane spanning regions: 2×10^{-10} cm^2/s (*41*) to 20×10^{-10} cm^2/s (*42*) for class I MHC molecules; 1.5×10^{-10} cm^2/s (*43*) to 6×10^{-10} cm^2/s (*44*) for EGF receptors. We note that the capacity for M5 to dimerize IL-1 RI may have influenced our measured values. A previous study showed that dimers of class I MHC molecules labeled with mAb yielded similar D values as those labeled with corresponding Fab fragments (*45*), as expected from the logarithmic dependence of D on the size of the laterally translating molecule (*39*). However, another study obtained significantly different values for class I MHC molecules labeled with intact mAb compared to their Fab fragments (*42*). The use of M5 Fab fragments in our measurements was precluded by their significant dissociation under the conditions of these experiments (unpublished results). The value of D for the mutant IL-1 RI which lacks the cytoplasmic tail is slightly less than that for the wild-type receptors transfected in to the same CHO cell line (Table 1), suggesting some influence of the cytoplasmic tail on the rate of lateral diffusion of the mobile receptors. IL-1 binding does not significantly alter the rate of lateral diffusion of the receptors that remain mobile as indicated by minimal effects on the value of D for either the tail-less mutant on the CHO cells or the wild-type receptor on either cell line.

Values for the mobile fraction (%R) for Cy3-M5-labeled IL-1 RI and the tail-less mutant are distributed broadly (Figure 1). This is reminiscent of FPR results for class I MHC molecules (*46*), and suggests heterogeneous interactions occur with other cell surface components and arise largely from interactions of the extracellular and/or transmembrane regions. The 14−18% decrease in the average value of %R observed after IL-1β binding for wild-type IL-1 RI on both the C-127 cells and the CHO cells suggests induced immobilization of this fraction of the occupied receptors. The tail-less mutant IL-1 RI shows a much smaller, statistically insignificant decrease in %R after IL-1 binding. This suggestion that the IL-1-dependent immobilization observed is largely due to interactions between the cytoplasmic tail and other cellular components may be related to the importance of the cytoplasmic tail in IL-1 RI-mediated signaling (*18*).

Consistent with the expected differences in sensitivity for rotational and lateral diffusion (*39*), we find that IL-1 causes large changes in the phosphorescence anisotropy decay of M5-labeled IL-1 RI under conditions for which lateral mobility changes are relatively small. The most obvious change in the phosphorescence anisotropy caused by IL-1 addition is an upward displacement of the decay curve to higher values of r_0 and r_∞ (Figure 3A,B). These simultaneous increases indicate a general reduction in the rotational freedom of the erythrosin probe. In addition, IL-1 causes a ∼2-fold increase in the rotational correlation time (ϕ) of the rotationally diffusing receptors that would be consistent with a ∼2-fold increase in molecular mass of these complexes.

The value of ϕ for ErITC-M5 bound to IL-1 RI in the absence of IL-1 is larger than expected for a single transmembrane protein in a fluid bilayer, or even for a dimer of this protein that may be created by bivalent M5. We previously found that the value of ϕ for IgE bound to FcϵRI, a receptor with seven transmembrane segments, was about

40 μs, similar to the value for M5-labeled IL-1 RI. Dimerization of IgE-FcϵRI on membrane vesicles by a mAb resulted in a 2-fold increase in the value of ϕ (*33*). Thus, if M5−IL-1 RI complexes are actually dimers of IL-1 RI, then ϕ for a single IL-1 RI would be expected to be ~20 μs, which is still much larger than the value of 2−3 μs predicted for a protein with a single transmembrane segment (*39*). This suggests that other transmembrane polypeptides are associated with IL-1 RI, even in the absence of IL-1, or that the bilayer in the vicinity of this receptor is correspondingly less fluid.

As previously described (*33*, *47*), the ratio of r_∞/r_0 provides a measure of the immobile fraction of receptors on the microsecond time scale. IL-1 binding causes a significant increase in this ratio from 0.60 to 0.78 (Table 2), suggesting that the fraction of the immobile M5−IL-1 RI complexes increases in response to IL-1 binding, consistent with the lateral diffusion measurements. The increase in r_0 that occurs with addition of IL-1 may result from a decrease in the segmental motion of the IL-1 RI-M5 complex; it could also represent a decrease in a population of IL-1 RI that rotates in the plane of the membrane with ϕ less than 5 μs. That changes in phosphorescence anisotropy are maintained after washing away readily dissociable IL-1 (Figure 3B) suggests the tightly bound IL-1 is responsible for the observed reduction in rotational mobility.

Our observation that IL-1 causes 10−20% of IL-1 RI to become associated with the detergent-resistant cellular residues may be another manifestation of ligand-induced interactions. Such insolubility in nonionic detergents such as Triton X-100 is also observed after aggregation of multichain immune recognition receptors, including B cell receptors (*48*), T cell receptors (*49*, *50*), and receptors for IgE (*51*, *52*), and appears to involve interactions with the actin cytoskeleton (*48*, *51*). We find that a small fraction of IL-1 RI is not solubilized with Triton X-100 in the absence of IL-1 ligands, and binding of IL-1 increases this fraction more than 2-fold at 22 °C with little or no increase at 4 °C (Figure 4B). This temperature dependence is similar to that observed with IL-1-mediated IL-1 RI aggregation and cell activation (*24*). IL-1 RI internalization precluded evaluation at 37 °C (unpublished results). The percentage increase in detergent insolubility of IL-1 RI in response to IL-1 is similar in magnitude to the percentage decrease in mobile fraction in response to IL-1 (Table 1), suggesting a direct relationship between these ligand-dependent changes. Furthermore, the requirement for the cytoplasmic tail of IL-1 RI for the loss of lateral mobility suggests that these chances reflect functionally important interactions with cytoskeletally anchored structures.

Our physical measurements are probably relevant to recent studies that indicate IL-1-dependent interactions between IL-1 RI and proteins involved in signaling (*12*, *53*, *54*). We evaluated the interesting case of IL-1ra. Although this ligand does not cause detectable signaling by IL-1 RI, single point mutations can convert it to a signaling ligand (*55*), suggesting that it may be structurally similar enough to IL-1 to cause some signaling steps that are insufficient for the complete response. Supporting this view are our biophysical data: IL-1ra causes a small increase in FRET when IL-1 RI is labeled with bivalent M5, but no significant change was observed in response to IL-1ra when IL-1 RI was labeled with M5 Fab fragments (*24*); IL-1ra causes a significant change in the phosphorescence anisotropy decay of ErITC-M5-labeled IL-1RI which is intermediate between that for unliganded receptor and that for receptor with IL-1α bound (Figure 3A); IL-1ra in the presence of M5 causes significant detergent insolubility of IL-1 RI at 22 °C but not 4 °C (Figure 4). These independent results indicate that bivalent binding by M5 can facilitate a significant change in the physical state of IL-1 RI in response to IL-1ra. These changes correlate with a small but significant production of arachidonic acid in response to IL-1ra in combination with M5 (*37*), providing further evidence that the physical properties we have characterized are relevant to signal transduction mediated by this receptor.

Our results support a model in which IL-1 binding causes self-aggregation of IL-1 RI, and this aggregation induces interactions with other cellular components that significantly reduce rotational mobility. This can lead to further interactions via the cytoplasmic segment of the receptors that cause loss of lateral mobility, detergent insolubility, and stimulation of signaling events. Furthermore, in the presence of the bivalent M5 mAb, IL-1ra may become a partial agonist, underscoring the importance of receptor aggregation in the initiation of signaling by this ubiquitous receptor.

ACKNOWLEDGMENT

We are grateful for the assistance of Dr. En-Yuh Chang in performing the phosphorescence anisotropy experiments. The FPR experiments were conducted at the National Institutes of Health−National Science Foundation Developmental Resource for Biophysical Imaging and Optoelectronics at Cornell, directed by Watt W. Webb.

REFERENCES

1. Rambaldi, A., Torcia, M., Bettoni, S., Vannier, E., Barbui, T., Shaw, A. R., Dinarello, C. A., and Cozzolino, F. (1991) *Blood 78*, 3248−3253.
2. Dinarello, C. A. (1994) *FASEB J. 8*, 1314−1325.
3. Dinarello, C. A. (1988) *FASEB J. 2*, 108−115.
4. Farrar, W. L., Mizel, S. B., and Farrar, J. J. (1980) *J. Immunol. 124*, 1371−1377.
5. Mizel, S. B., Dayer, J. M., Krane, S. M., and Mergenhagen, S. E. (1981) *Proc. Natl. Acad. Sci. U.S.A. 78*, 2474−2477.
6. March, C. J., Mosley, B., and Larsen, A. (1985) *Nature 315*, 641−647.
7. Saklatvala, J., Sarsfield, S. J., and Townsend, T. (1985) *J. Exp. Med. 162*, 1208−1222.
8. Vigers, G. P. A., Caffes, P., Evans, R. J., Thompson, R. C., Eisenberg, S. P., and Brandhuber, B. J. (1994) *J. Biol. Chem. 269*, 12874−12879.
9. Heguy, A., Baldari, C., Bush, K., Nagele, R., Newton, R. C., Robb, R. J., Horuk, R., Telford, J. L., and Melli, M. (1991) *Cell Growth. Differ. 2*, 311−316.
10. Sims, J. E., Gayle, M. A., Slack, J. L., Alderson, M. R., Bird, T. A., Giri, J. G., Colotta, F., Re, F., Mantovani, A., and Shanebeck, K. (1993) *Proc. Natl. Acad. Sci. U.S.A. 90*, 6155−6159.
11. Stylianou, E., O'Neill, L. A. J., Rawlinson, L., Edbrooke, M. R., Woo, P., and Saklatvala, J. (1992) *J. Biol. Chem. 267*, 15836−15841.
12. Wesche, H., Henzel, W. J., Shillinglaw, W., Li, S., and Cao, Z. (1997) *Immunity 7*, 837−847.
13. Sims, J. E., Acres, R. B., Grubin, C. E., McMahan, C. J., Wignall, J. M., March, C., and Dower, S. K. (1989) *Proc. Natl. Acad. Sci. U.S.A. 86*, 8946−8950.

14. Sims, J. E., March, C. J., Cosman, D., Widmer, M. B., MacDonald, H. R., McMahan, C. J., Grubin, C. E., Wignall, J. M., Jackson, J. L., Call, S. M., Friend, D., Alpert, A. R., Gillis, S., Urdal, D. L., and Dower, S. K. (1988) *Science 241*, 585−589.
15. McMahan, C., Slack, J. L., Mosley, B., Cosman, D., Lupton, S. D., Brunton, L. L., Grubin, C. E., Wignall, J. M., Jenkins, N. A., Brannan, C. I., Copeland, N. G., Huebner, K., Croce, C. M., Cannizzarro, L. A., Benjamin, D., Dower, S. K., Spriggs, M. K., and Sims, J. E. (1991) *EMBO J. 10*, 2821−2832.
16. Kubota, K., Keith, F. J., and Gay, N. J. (1993) *Biochem. J. 296*, 497−503.
17. Hanks, S. K., Quinn, A. M., and Hunter, T. (1988) *Science 241*, 42−52.
18. Curtis, B. M., Gallis, B., Overell, R. W., McMahan, C. J., Deroos, P., Ireland, R., Eisenman, J., Dower, S. K., and Sims, J. E. (1989) *Proc. Natl. Acad. Sci. U.S.A. 86*, 3045−3049.
19. Leung, K., Betts, J. C., Xu, L., and Nabel, G. J. (1994) *J. Biol. Chem. 269*, 1579−1582.
20. Heguy, A., Baldari, C. T., Censini, S., Ghiara, P., and Telford, J. L. (1993) *J. Biol. Chem. 268*, 10490−10494.
21. Croston, G. E., Cao, Z., and Goeddel, D. V. (1995) *J. Biol. Chem. 270*, 16514−16517.
22. Chin, J., Cameron, P. M., Rupp, E., and Schmidt, J. A. (1987) *J. Exp. Med. 165*, 70−86.
23. Greenfeder, S. A., Nunes, P., Kwee, L., Labow, M., Chizzonite, R. A., and Ju, G. (1995) *J. Biol. Chem. 270*, 13757−13765.
24. Guo, C., Dower, S. K., Holowka, D., and Baird, B. (1995) *J. Biol. Chem. 270*, 27562−27568.
25. Dower, S. K., Kronheim, S., March, C. J., Conlon, P. J., Gillis, S., Hopp, T. P., and Urdal, D. L. (1985) *J. Exp. Med. 162*, 501−515.
26. Gallis, B., Prickett, K. S., Jackson, J., Slack, J., Schooley, K., Sims, J. E., and Dower, S. K. (1989) *J. Immunol. 143*, 3235−3240.
27. Bird, T. A., Schule, H. D., Delaney, P. L., Sims, J. E., Thoma, B., and Dower, S. K. (1992) *Cytokine 4*, 429−440.
28. Dower, S. K., Wignall, J. M., Schooley, K., McMahan, C. J., Jackson, J. L., Prickett, K. S., Lupton, S., Cosman, D., and Sims, J. E. (1989) *J. Immunol. 142*, 4314−4320.
29. Segal, D. M., and Hurwitz, E. (1977) *J. Immunol. 118*, 1338−1347.
30. Thomas, J. L., and Webb, W. W. (1990) in *Noninvasive Techniques in Cell Biology* (Ginstein, S., and Fokett, K., Eds.) pp 129−152, Wiley-Liss, New York.
31. Yguerabide, J., Schmidt, J. A., and Yguerabide, E. E. (1982) *Biophys. J. 40*, 69−75.
32. Chang, E. Y., Mao, S. Y., Metzger, H., Holowka, D., and Baird, B. (1995) *Biochemistry 34*, 6093−6099.
33. Myers, J. N., Holowka, D., and Baird, B. (1992) *Biochemistry 31*, 567−575.
34. Myers, J. N. (1991) Ph.D. Thesis, Cornell University, Ithaca, NY.
35. Jovin, T. M., and Vaz, W. L. C. (1989) *Methods Enzymol. 172*, 471−513.
36. Bomsztyk, K., Sims, J. E., Stanton, T. H., Slack, J., McMahan, C. J., Valentine, M., and Dower, S. K. (1989) *Proc. Natl. Acad. Sci. U.S.A. 86*, 8034−8038.
37. Guo, C. (1996) Ph.D. Thesis, Cornell University, Ithaca, NY.
38. Edidin, M. (1987) *Curr. Top. Membr. Transp. 29*, 91−125.
39. Saffman, P. G., and Delbruck, M. (1975) *Proc. Natl. Acad. Sci. U.S.A. 72*, 3111−3113.
40. Mastin, M., Bol, G. F., Ericksson, A., Reoch, K., and Brigelius-Flohe, R. (1994) *Eur. J. Immunol. 24*, 1366−1371.
41. Barbour, S., Edidin, M., Felding-Habermann, B., Taylor-Norton, J., Radin, N. S., and Fenderson, B. A. (1992) *J. Cell. Physiol. 150*, 610−619.
42. , Bierer, B. E., Herrmann, S. H., Brown, C. S., Burakoff, S. J., and Golan, D. E. (1987) *J. Cell Biol. 105*, 1147−1152.
43. Livneh, E., Benveniste, M., Prywes, R., Felder, S., Kam, Z., and Schlessinger, J. (1986) *J. Cell Biol. 103*, 327−331.
44. Zidovetzki, R., Yarden, Y., Schlessinger, J., and Jovin, T. M. (1981) *Proc. Natl. Acad. Sci. U.S.A. 78*, 6981−6985.
45. Wier, M., and Edidin, M. (1988) *Science 242*, 412−414.
46. Edidin, M., and Wei, T. (1982) *J. Cell Biol. 95*, 458−462.
47. Kawato, S., and Kinosita, K., Jr. (1981) *Biophys. J. 36*, 277−296.
48. Braun, J., Hochman, P. S., and Unanue, E. R. (1982) *J. Immunol. 128*, 1198−1204.
49. Marano, N., Holowka, D., and Baird, B. (1989) *J. Immunol. 143*, 931−938.
50. Geppert, T. D., and Lipsky, P. E. (1991) *J. Immunol. 146*, 3298−3305.
51. Robertson, D. R., Holowka, D., and Baird, B. (1986) *J. Immunol. 136*, 4565−4572.
52. Apgar, J. (1990) *J. Immunol. 145*, 3814−3822.
53. Huang, J., Gao, X., and Cao, Z. (1997) *Proc. Natl. Acad. Sci. U.S.A. 94*, 12829−12832.
54. Reddy, S. A. G., Huang, J. H., and Liao, W. S.-L. (1997) *J. Biol. Chem. 272*, 29167−29173.
55. Ju, G., Labriola-Tompkins, C. C., Campen, C. A., Benjamin, W. R., Karas, J., Plocinski, J., Biondi, D., Kaffka, K. L., Kilian, P. L., Eisenberg, S. P., and Evans, R. J. (1991) *Proc. Natl. Acad. Sci. U.S.A. 88*, 2658−2662.

BI982068L